JOURNAL OF NATURAL REMEDIES
DOI: 10.18311/jnr/2024/43768
RESEARCH ARTICLE

Identification of Flavonoids-based HITS To Inhibit GSK3β Activity: An *In Silico* and *In Vitro* Analysis

Muthiah Ramanathan[1*], Vijayalakshmi Chinniah[2] and S. E. Maida Engels[3]

[1]Department of Pharmacology, PSG College of Pharmacy, Peelamedu, Coimbatore - 641004, Tamil Nadu, India; muthiah.in@gmail.com

[2]Department of Pharmacognosy, PSG College of Pharmacy, Peelamedu, Coimbatore - 641004, Tamil Nadu, India

[3]Department of Pharmaceutical Chemistry, PSG College of Pharmacy, Peelamedu, Coimbatore - 641004, Tamil Nadu, India

Abstract

Background: Glycogen synthase kinase-3 (GSK-3) is a protein kinase with two isoforms, alpha and beta. GSK-3β, specifically, is found in nervous tissue and has been linked to the development of various human diseases. **Aim:** This study aimed to investigate the potential of flavonoids as inhibitors of GSK-3β using *in silico* and *in vitro* analyses. **Methods:** Schrodinger Maestro software was used for *in silico* molecular docking simulations to assess the interaction between flavonoids (ligands) and GSK-3β (target protein). *In vitro* cytotoxicity studies were performed on Rat L6 skeletal muscle cells to determine the safety of the selected flavonoids. Additionally, the neuroprotective effects of the flavonoids were evaluated using an oxygen-glucose deprivation model on SHSY 5Y neuroblastoma cells. **Results:** The *in silico* analysis revealed that all the studied flavonoids interacted with valine 135, a key amino acid for GSK-3β inhibition. Furthermore, the *in vitro* studies showed that the selected flavonoids were safe up to a concentration of 30 µM in rat L6 cells. Among the tested flavonoids, hesperetin, a flavanone, demonstrated the most potent neuroprotective effect in the SHSY 5Y cell line, with an IC50 value of 13.30 µM. **Conclusion:** Hesperetin, a flavanone, emerged as the most promising candidate among the tested flavonoids for further investigation as a potential GSK-3β inhibitor with neuroprotective properties.

Keywords: Cytotoxicity, Hesperetin, Oxygen-Glucose Deprivation, Neuroblastoma, Valine 135

Abbreviations: ADME- Absorption, Distribution, Metabolism, Excretion; ATP- Adenosine Tri Phosphate; FBS- Fetal Bovine Serum; GSK -Glycogen synthase kinase-3; NCCS- National Centre for Cell Science; NPT- Normal Pressure and Temperature; OGD- Oxygen Glucose Deprivation; OPLS- Optimized Potentials for Liquid Simulations; PDB- Protein Data Bank PSA- Polar surface area; SASA- Solvent Accessible Surface Area

1. Introduction

Flavonoids fascinated a wide range of researchers in recent years due to their numerous therapeutic potential[1]. Flavonoids are polyphenolic compounds found to be present abundantly in fruits, vegetables, grains, herbs, spices, and beverages[2,3]. Flavonoids consist of 15 carbon atoms arranged in a three-ring structure synthesized through the phenylpropanoid metabolic pathway (C6–C3–C6). Flavonoids are categorized into different groups such as flavones, flavanones, isoflavones, flavonols, and anthocyanins etc. based on factors like their chemical structure, degree of unsaturation, and oxidation of the carbon ring[4,5].

The antioxidant profile of flavonoids, particularly their presence in the brain *in vivo*, plays a crucial role in expressing the neuroprotective capacity. It is well established that metabolic transformations, such as glucuronidation and methylation, are common, resulting in only a very small number of flavonoids in their aglycone form in the blood[6,7]. Additionally, the polar nature of flavonoids limits their permeability through the blood-brain barrier, presenting an added obstacle to their ability to reach the brain[8].

*Author for correspondence

Article Received on: 22.10.2022 Revised on: 21.08.2023 Accepted on: 16.09.2023

Inhibition of GSK3β activity may result in a decrease in glycogen synthesis from glucose[9]. This enzyme is consistently active and widely expressed in various body tissues, especially in neurons[10,11] and glia[12]. GSK3β is now known to control numerous cellular processes via different signalling pathways crucial for cell growth, programmed cell death, and growth. Due to its diverse functions, the malfunction of this kinase is linked to the development of several human diseases, including nervous system disorders, diabetes, bone formation problems, inflammation, cancer, and heart failure. GSK3β is present in all brain regions with varying levels of mRNA[13] and is observed to be increased in neurodegenerative diseases. AR-A014418, a specific and potent GSK3β inhibitor, has been shown to clear Aβ by phosphorylating GSK3β at S9 and activating the mTOR pathway in a mouse model. GSK3β has also been associated with the downstream effects of β-amyloid. Exposure of cortical and hippocampal primary neuronal cultures to β-amyloid[14] triggers the activation of GSK3β[15] and cell death[16,17]. Blocking GSK3β expression with antisense oligonucleotides or inhibiting its activity with lithium[18] prevents Aβ-induced neurodegeneration in cortical and hippocampal primary cultures. Research indicates that natural compounds like flavonoids have strong potential as preventive and therapeutic measures against various neurodegenerative conditions. Therefore, understanding the neuroprotective capabilities of flavonoids will not only enhance brain resilience against neurodegeneration but also promote overall brain health. The multifaceted actions of different types of flavonoids, including antioxidative[19,20] and anti-inflammatory properties[21], and their ability to modulate mitochondrial support and neurotransmitter systems[8], contribute to promoting neuron survival and cognitive function[22]. Consequentially, the study emphasizes the role of GSK-3β in neurodegenerative diseases like Alzheimer's. However, existing GSK-3β inhibitors, primarily delivered through injections, limit their use for these neurodegenerative conditions. Furthermore, none have yet been approved for clinical use. This research addresses these limitations by focusing on *in silico* screening to identify potential flavonoid "hits" that can inhibit GSK-3β.

2. Materials and Methods

2.1 Protein Preparation

The Glycogen Synthase Kinase (GSK-3β) crystal structure bound to inhibitor AR-A014418 was retrieved from the RCSB Protein Data Bank (PDB ID: 1Q5K) at a resolution of 1.94 Å[23]. The protein consists of 689 amino acid residues (5521 protein atoms), two bound inhibitors (42 atoms), 373 water molecules, and two GSK3β molecules, each with a bound inhibitor[24]. Protein refinement was completed through the utilization of the protein preparation tool[25] of Maestro. The process of protein preparation involves four essential steps: import, preprocessing, review, and modification and refinement. To minimize strain, heavier atoms were constrained through an energy minimization process using OPLS_2005. Establishing the receptor grid is crucial when the protein is bound to the ligand. During this stage, the molecule linked to the protein structure was utilized to define both the internal and external receptor grid boxes. OPLS_2005 served as the force field energy during the receptor grid formation. Penalties were mitigated by implementing a Vander wall radius scaling and partial charge cutoff value for non-polar atoms.

2.2 Ligand Preparation

The 2D structures of flavonoids like rutin, hesperidin, apigenin, galangin, isovitexin, and hesperetin were downloaded from the PubChem database and shown in Figure 1. The LigPrep module of Schrodinger Maestro 2023-1 generates potential stereoisomers, tautomers, and states at physiological pH or any other user-defined pH in addition to converting the 2D chemical structure into a 3D energy-minimized molecular structure.

2.3 Molecular Docking Studies

GLIDE v9.8 was employed for the ligand-receptor docking analysis. All ligands that were docked were confined within the grid-defined area of the protein structure. Ligands containing more than 300 atoms and 50 charges were not considered in the study. The partial charge cut-off was set at 0.15, while the Van der Waals scaling factor remained at the default value of 0.80[26]. The best poses were chosen after post-docking refinement using the docking score/ eModel score. The equation for Gscore is calculated by summing up

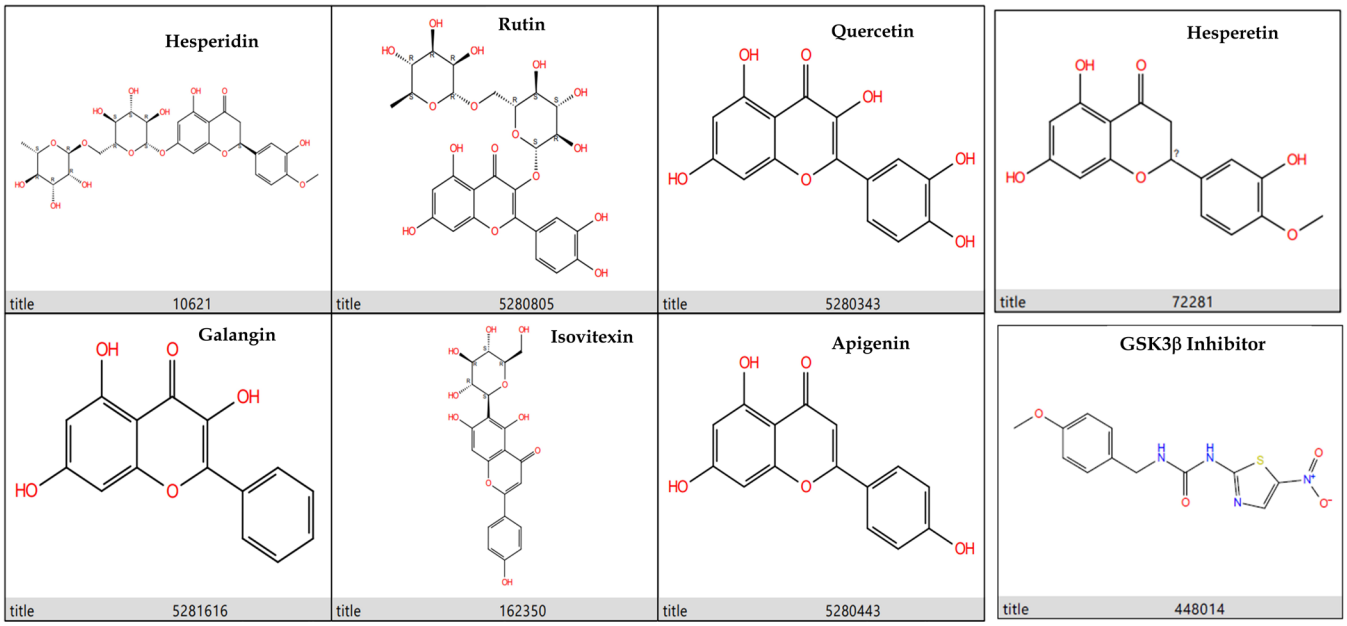

Figure 1. Ligand structure with their PubChem ID.

the contributions from various factors. These factors include 0.05 times the Van der Waals interaction energy (vdW), 0.15 times the Coulombic interaction energy (Coul), the lipophilic interaction energy (lipo), the hydrogen bonding energy (Hbond), the metal interaction energy (Metal), the reward term (Reward), the number of rotatable bonds (RotB), and the site-specific energy contribution (Site)[27]. The glide score, determined by the XP scoring method, contributes to the docking score, while the eModel score evaluates the "favorability" of a docked complex[28].

2.4 ADME Prediction using QikProp v7.5

The QikProp tool from Maestro v13.5 was utilized to analyze the preliminary ADME properties of the chosen ligands. Schrödinger QikProp v7.5 was employed to predict ADME properties. QikProp offers a range of important characteristics to comprehend absorption, distribution, metabolism, excretion, and toxicity (ADME/tox)[29]. These descriptors encompass forecasted blood-brain barrier permeability (logBB), Polar Surface Area (PSA), partition coefficient, PMDCK cell permeability, projected apparent Lipinski rule of five violations, projected Jorgensen rule of three violations, anticipated CNS activity, and anticipated IC50 value of ether-a-go-go related gene k^+ channel blockage (logHERG). Lipinski's rule of five includes molecular weight, number of hydrogen bond donors, number of hydrogen bond acceptors, and expected octanol-water partition coefficient, indicating the probability of a chemical acting as a drug. Jorgensen's rule of three, which considers forecasted Caco-2 cell permeability, anticipated aqueous solubility (logS), Solvent Accessible Surface Area (SASA), and the number of likely metabolic reactions, describes the bioavailability of orally active medications.

2.5 Molecular Dynamics

To assess the stability of complex formation in a biologically inspired environment, a molecular dynamics simulation was conducted using DESMOND V5.2. The complexes included in the simulation were solvated in orthorhombic boxes[1] using the TIP3P model[1]. To balance the system, counterions like Na+ and Cl- ions were introduced with a salt concentration of 0.15M. The OPLS_2005 force field[7] was then applied to relax the system. After undergoing multiple energy minimization stages, the equilibrated system underwent a 100 ns simulation using the NPT ensemble class to investigate the intricate dynamics of the small molecule during its interaction. The resulting MD trajectory was analyzed using various metrics, including protein-ligand –root mean square deviation, sum of squared residuals, root mean square fluctuation, % protein-ligand interactions, and ligand torsion profile. The

stability of complex formation was evaluated and compared to co-crystal complexes[30].

2.6 *In Vitro* Studies Cytotoxic Studies

The toxicity level of the selected phytomolecules towards the L6 skeletal muscle cell line[31] was evaluated using the MTT assay. The Rat L6 skeletal muscle cell line, obtained from NCCS, Pune, was cultured in DMEM growth media containing phenol red as an indicator. The assay was carried out in a 96-well plate, with the cells seeded at a density of 5000 cells per well and incubated at 37°C and 5% CO2 in a thermo scientific incubator[32]. After 24 hours, the cells were treated with various concentrations (0.3, 1, 10, 20, 30 µM) of lead molecules and a standard solution dissolved in dimethyl sulphoxide. Following 48 hours, the media was removed, and the cells were treated with 10 µl of MTT[33], then incubated for 4 hours. To measure absorbance at 570 nm, 100 µl of DMSO was added to dissolve the formed formazan crystals[34]. The statistical analysis was conducted using the software Graphpad Prism 8.0.2.

2.7 Differentiation of SHSY-5Y Neuroblastoma Cell Line

The SHSY-5Y subcloned cell line derived from human neuroblastoma was acquired from NCCS located in Pune. By gradually depriving these cells of serum and supplementing them with retinoic acid[35,36], they can change from having an epithelial phenotype to having a neuronal phenotype. It has been demonstrated that various markers found in mature neurons, such as GAP43, NeuroD2, and NgN[37,38] develop in a completely differentiated neuron. We followed a seven-day differentiation strategy that was well-documented and optimized in our lab. The Fetal Bovine Serum (FBS; Gibco), was added to DMEM nutrient media as a supplement. Cells were kept in a humid atmosphere at 37°C and 5% CO2[39]. Every three days, the medium was changed. 10M of retinoic acid was added to the growth medium to start the differentiation process. Trypsinization was carried out at short intervals to enrich the neuronal cell. With gradual serum depletion in the media, a seven-day differentiation technique is used. Due to the significant connection of gene expression between neuronal markers including GAP43, NgN1, and NeuroD2, a seven-day strategy was chosen[40,41].

2.8 *In Vitro* Neuroprotective Effect by Oxygen-Glucose Deprivation

The study used the Oxygen-Glucose Deprivation (OGD) paradigm to simulate an ischemic insult. To mimic the condition, Nacl (120mM), Kcl (5mM), CaCl2 (1.2mM), KH2PO4 (1.1mM), MgSO4 (1.2mM) and NaHCO3 (20mM) was used in the medium[42]. The cells were kept in a prefilled hypoxic chamber with 5% carbon dioxide and 95% nitrogen gas to accomplish OGD. Before two hours of ischemia injury, the lead molecules were pre-treated on the cells. Ischemic insult was performed for 20 minutes, followed by a re-perfusion of growth media (1% FBS) and a 48-hour incubation period with various medication doses. Cell viability was evaluated using an MTT test after 48 hours of cell observation[43].

3. Results and Discussion

3.1 Molecular Docking Studies

GSK3β enzyme contains three distinct regions within its ATP binding site that play a crucial role in determining the effectiveness of inhibitory molecules. These regions include specific amino acid residues such as Tyr 134, Asp133, and Val135 in the hinge region, Gly63, Ile62, Val70, and Phe67 in a hydrophobic pocket, and Glu97, Lys 85, Glu185, Arg141, Asp200, and Cys199 in a polar region. The inhibitory properties and selectivity of GSK3β are influenced by the interaction of these amino acid residues with at least two of these regions. Molecules that interact with amino acid residues in either the polar region or the hydrophobic pocket region determine the selectivity and potency of the inhibitor. Well-known selective and potent GSK3β inhibitors typically interact with amino acid residues such as Val135, Asp133, Arg141, Glu137, Asp200, Arg220, and Gln185. Additionally, amino acids like Tyr 134 contribute to hydrophobic interactions, while Arg141 facilitates cationic or ionic interactions with inhibitor molecules that occupy a hydrophobic pocket formed by the gatekeeper residue Leu132. All the selected flavonoid phytomolecules were screened against the target protein 1Q5K. The results of the glide G score were observed in the order Isovitexin> Rutin>Quercetin>Hesperidin>Apigenin>Galangin>Hesperetin. The interaction of the selected ligands was compared with that of standard GSK 3β. Inhibitor AR-A014418 Inhibitor VIII. The major interaction was found to be with amino acid valine 135 which was the predominant interaction in all the major

GSK3β inhibitors and the interactions were tabulated in Table 1 and Figure 2.

3.2 ADME Properties

The treatment of thiazole molecule AR-A014418 was reported to reduce the tau photophosphorylation in cells but exhibited poor physicochemical properties due to which it has been discontinued from clinical usage. The ADME characteristics of flavonoids were studied to understand the drug-likeness of the phytomolecule and the results were given in Table 2. The percentage of human oral absorption

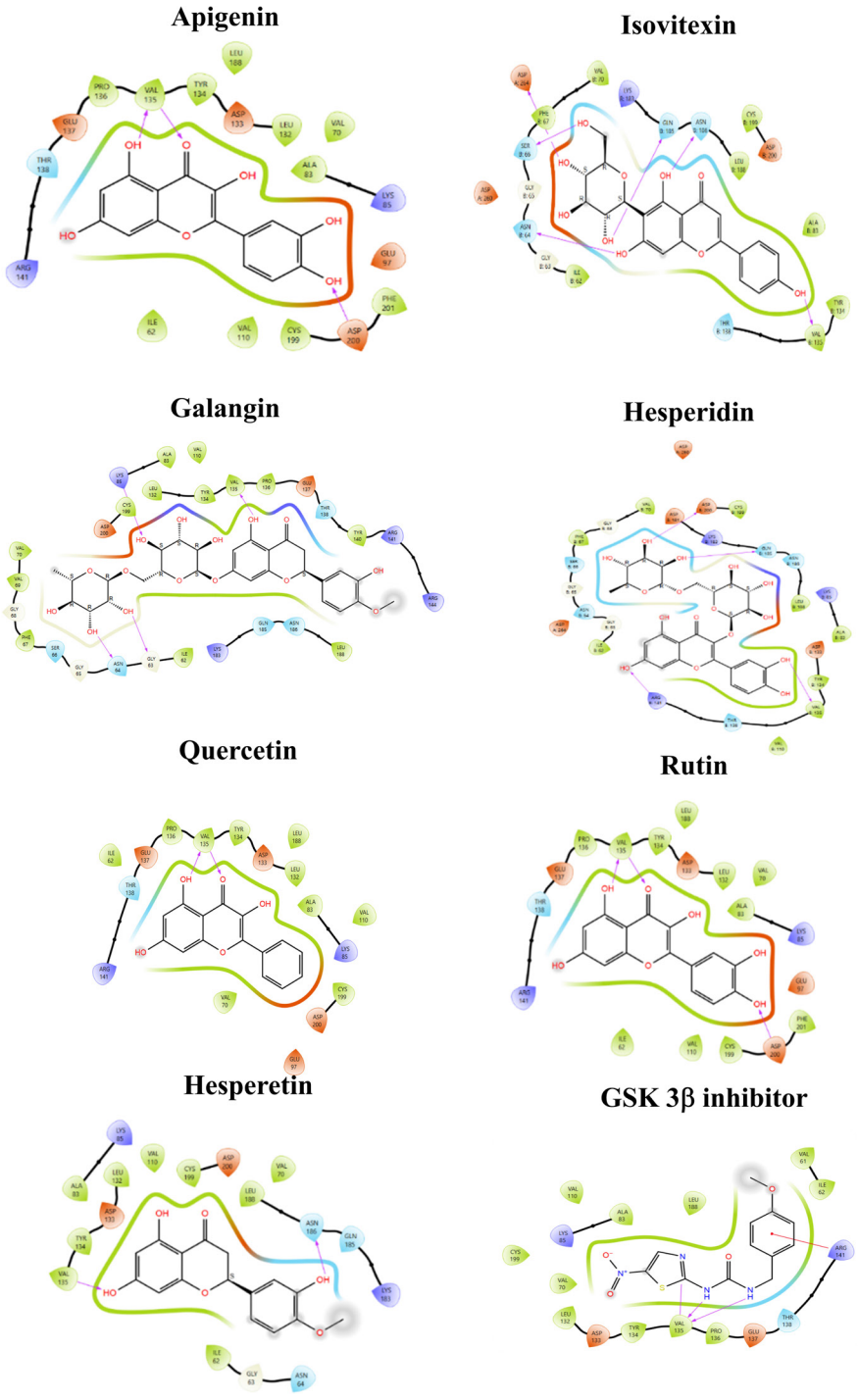

Figure 2. Protein-ligand interaction.

of hesperetin (61.586%), Apigenin (73.5%) and galangin (77.72%) are in the moderate range when compared to other flavonoids. Polar surface area is a crucial descriptor representing the total surface area of the molecule that is polar which can form an H-bond interaction.

3.3 Molecular Dynamics

Molecules with higher oral absorption rates (> 60 – moderate) were further analyzed for their molecular dynamics properties. In the molecular dynamics study, the simulation trajectory was maintained for 100 nanoseconds. The Root-Mean-Square Deviation (RMSD) of the GSK3β complex with hesperetin, which remained more constant with the target protein throughout the 100 ns duration, and the standard GSK3β inhibitor are shown in Figure 3A-D. The RMSD for the protein began at 1.2 Å and constant around 2 Å for the ligand. In contrast, the RMSD for the standard started at 1.5 Å, while the ligand began at 0.6 Å. For small globular proteins, RMSD fluctuations within the 1–3 Å range are acceptable, with changes greater than 3 Å indicating significant conformational changes that are not preferable. The interaction of hesperetin and the standard with GSK3β remained stable throughout the 100 ns. The oxygen atoms in the benzopyran scaffold of hesperetin displayed hydrogen bond interactions with VAL 135 (93% and 99%). In the C ring, hydrogen bonds were formed with LYS 85 (92% for the -OH group, 85% for the -OCH_3 group), ASP 200 (35%), and ARG 141, bridged with H_2O (30%), as shown in Figure 3E-H. For the GSK3β inhibitor AR-A014418 (Inhibitor VIII), the major interaction was with VAL 135 (75%).

Table 1. Glide G-score and ligand interaction

Compound	Docking score	Ligand interaction
Apigenin	-9.396	H-bond - Val 135, Asp 200
Isovitexin	-12.78	H-bond - Asp 264, Ser 66, Asn 64, Gln 185, Asn 186, Val 135
Galangin	-9.297	H-bond -Val-135
Quercetin	-10.678	H-bond - Val 135, Asp 200
Rutin	-12.329	H-bond - Asp 200, Gln 185, Val 135, Arg 141
Hesperidin	-10.434	H-bond - Val 135, Lys 85, Gly 63, Asn 64
Hesperetin	-8.769	Val 135, Asn 186
GSK 3β inhibitor AR-A014418 (Inhibitor VIII)	-7.359	Pi cation-Arg 141; H-Bond –Val 135

Table 2. QikProp ADME properties

Descriptor and Range	AR-A014418	Hesperidin	Rutin	Quercetin	Galangin	Isovitexin	Apigenin	Hesperetin
mol_MW (130-725)	308.058	610.568	610.524	302.24	270.241	432.383	270.241	302.283
SASA (300-1000)	432.340	913.112	835.038	517.557	494.17	674.254	491.667	398.794
Donor HB (0-6)	2	7	9	4	2	6	2	2
accptHB (2-20)	7	20.05	20.55	5.25	3.75	12.25	3.75	4.25
QPlogPo/w (-2-6.5)	-0.314	-1.349	-2.695	0.385	1.799	-0.56	1.632	0.497
QPlogS (-6.5-0.5)	-0.269	-3.739	-2.605	-2.884	-3.399	-3.317	-3.357	-1.764
QPlogHERG (Concern below -5)	-3.891	-6.398	-5.757	-5.075	-5.29	-5.725	-5.137	-3.37
QPPCaco (<25 poor, >500 great)	417.702	2.894	0.368	19.269	177.21	8.728	116.772	313.895
QPlogBB (-3-1.2)	-0.739	-4.685	-5.29	-2.38	-1.282	-3.165	-1.441	-0.9
QPPMDCK (<25 poor, >500 great)	215.487	0.892	0.096	6.926	76.217	2.943	48.557	141.395
Percent Human Oral Absorption (>80 high, <25 poor)	2	0	0	52.194	77.721	27.549	73.5	61.586
PSA (7-200)	71.666	239.974	270.733	142.684	98.61	185.795	99.664	63.813
Rule of Three (Max 3)	0	2	2	1	0	2	0	0
Rule of Five (Max 4)	0	3	3	0	0	1	0	1

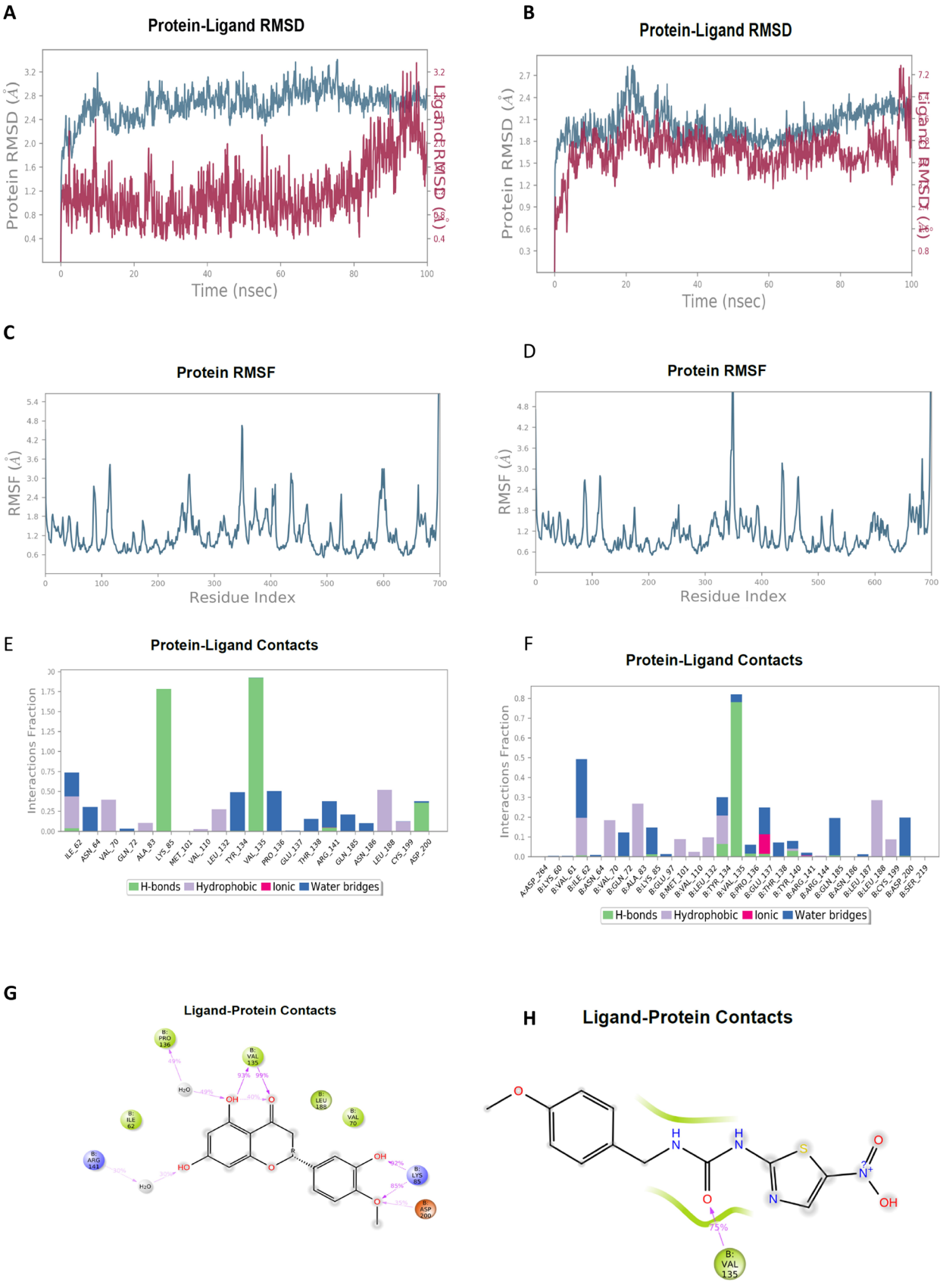

Figure 3. Molecular dynamics of hesperetin and standard GSK 3β inhibitor.

3.4 Cytotoxicity Studies

The *in vitro* cytotoxicity study of the selected flavonoids was carried out in rat L6 skeletal muscles. The morphology of the cell line after reaching 80% confluency is shown in Figure 4. The MTT assay revealed that all the selected phytomolecules were safer up to the concentration 30μM.

3.5 Neuroprotective Effect

After 7 days of RA treatment, the SHSY 5Y cell line underwent neuronal differentiation resulting in the formation of dendrites, as depicted in Figure 5B. Figure 5A, on the other hand, illustrates the normal cellular morphology of the SHSY 5Y cell line. Among various targets, GSK 3β was notably active under ischemic conditions. The downregulation of GSK 3β post-translational phosphorylation, along with downstream signalling proteins, contributed to the propagation of neurodegeneration during oxygen-glucose deprivation. Treatment with GSK3β inhibitors led to enhanced phosphorylation, indicating that the inhibitor could maintain GSK3β in an inactive state and prevent protein phosphatase 2A-mediated dephosphorylation.

Oxidative stress can stimulate Aβ production, aggregation, and tau protein phosphorylation, potentially initiating a harmful pathogenic cycle. The polyphenolic properties of flavonoids are crucial in managing neurodegenerative diseases due to their ability to scavenge free radicals. The presence of an aromatic ring with hydroxyl groups facilitates hydrogen and

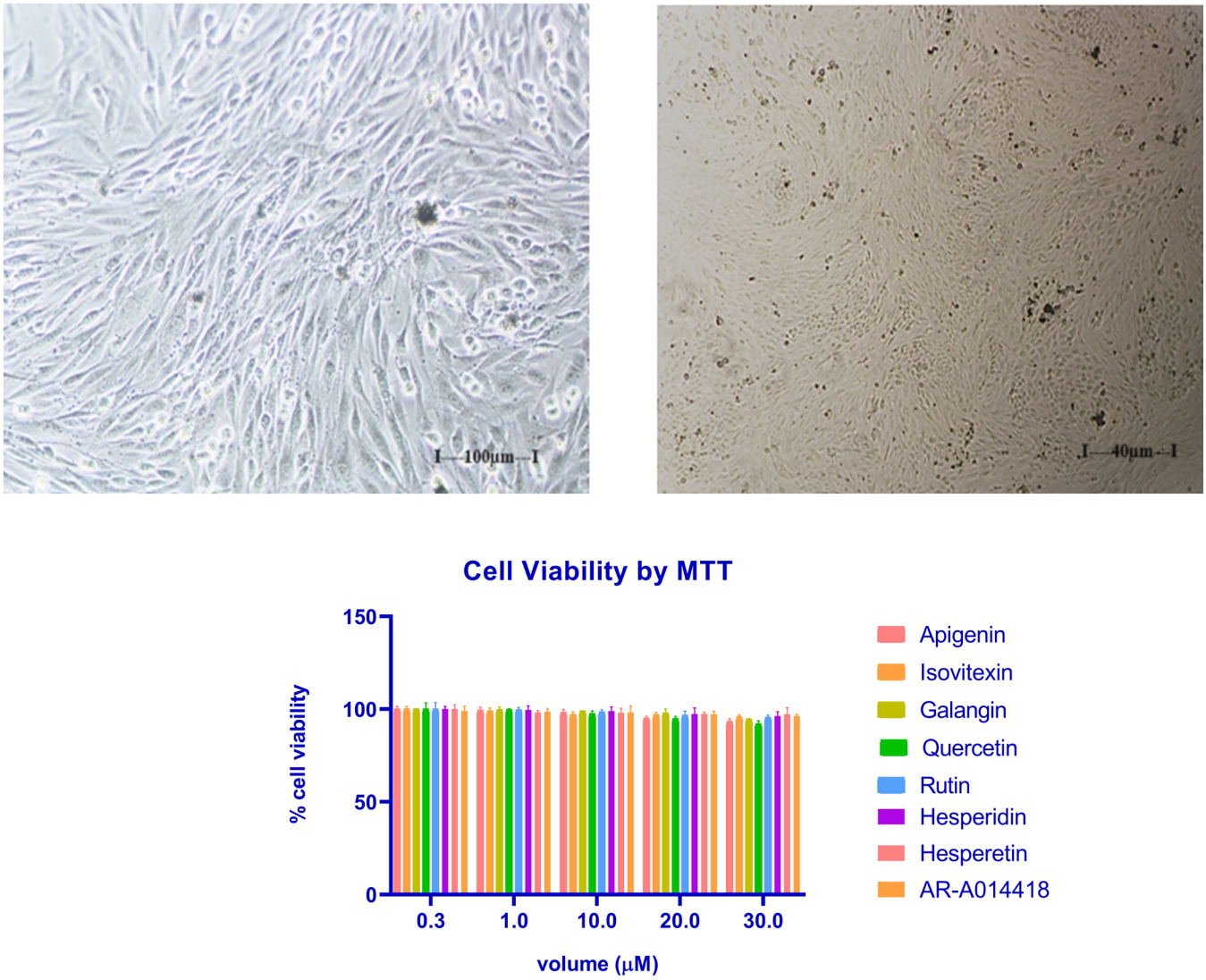

Figure 4. Cytotoxicity studies in rat L6 skeletal muscle.

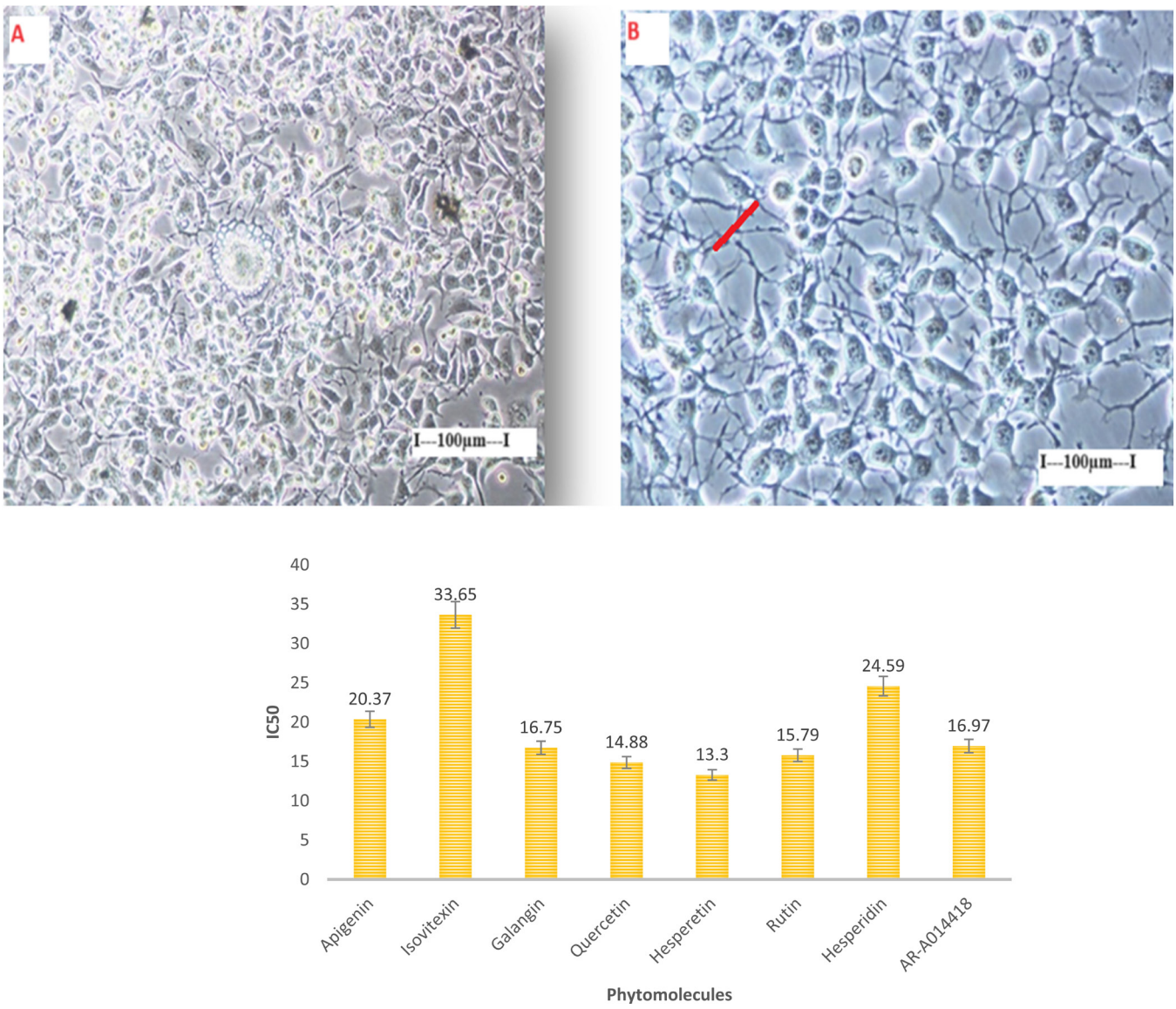

Figure 5. Neuroprotective effect in SHSY 5Y cell line by OGD model.

hydrophobic interactions, inhibiting fibril formation. Moreover, an increase in the number of hydroxyl groups on the aromatic ring enhances the anti-amyloidogenic properties. The positioning of the hydroxyl group at the 7th position of flavanone, as depicted in Figure 6, may promote GSK3β inhibitory activity and improve human oral absorption. Additionally, the methoxy group at the 3' position in the C-Ring of the flavanone nucleus enhances neuroprotection compared to other flavonoids studied. Polarity assessments and ADME calculations support hesperetin as a promising molecule. The neuroprotective effects of flavanone were validated through *in vitro* studies, with hesperetin exhibiting an IC50 value of 13.30 µM.

4. Conclusion

In the current study, molecular docking and *in vitro* assays were used to determine the potential hit molecule of GSK3β. The molecular docking analysis is confirmed by the binding affinities of the ligand and the precise interaction simulations of molecular dynamics. Among the flavonoids analysed hesperetin was found to be a better GSK 3β inhibitor compared to the standard AR-A014418. To develop a more potent GSK-3β inhibitor with therapeutic potential, **lead optimization strategies can be employed to modify the hesperetin molecule**. Building on this foundation, further structural modifications can be explored to

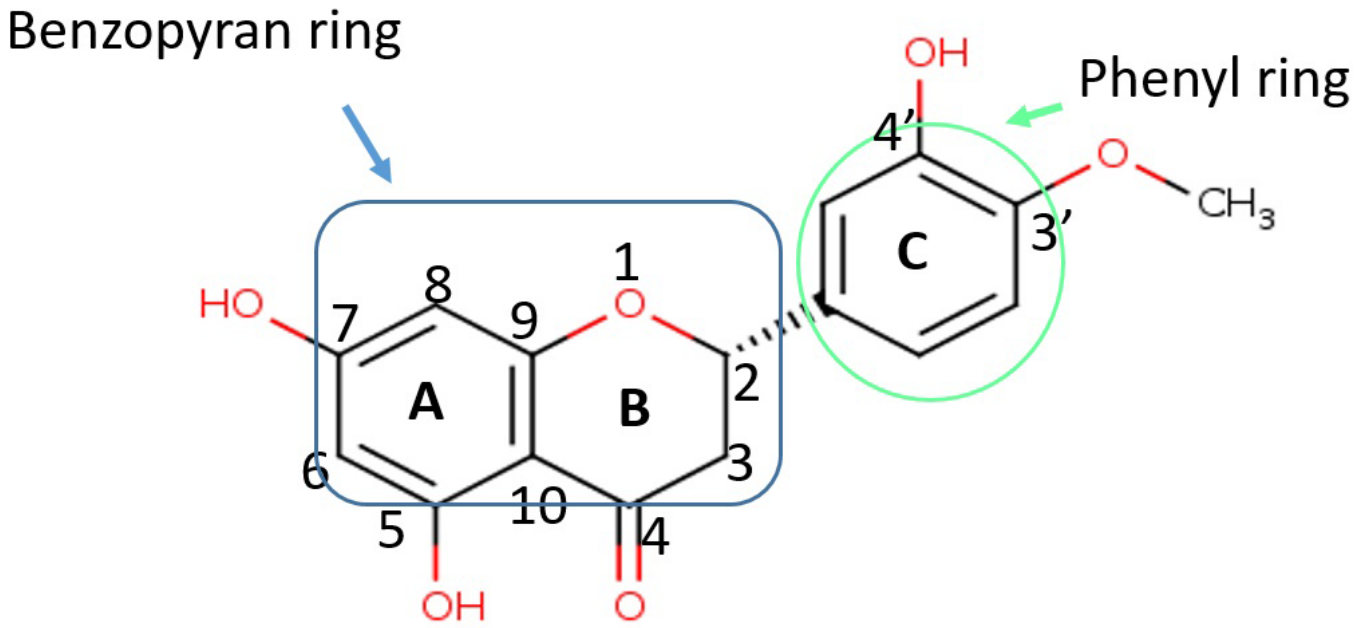

Figure 6. SAR of flavanone.

create an even more effective neuroprotective agent. Subsequently, the efficacy and safety of the optimized hesperetin derivatives can be rigorously evaluated in animal models of neurodegenerative diseases, which will pave the way for potential clinical applications.

5. Acknowledgement

The work is a part of the Ph.D. thesis of the Tamil Nadu, and authors are thankful to Dr. M. G. R. Medical University, Chennai.

6. References

1. Ullah A, Munir S, Badshah SL, Khan N, Ghani L, Poulson BG, Emwas AH, Jaremko M. Important flavonoids and their role as a therapeutic agent. Molecules. 2020; 25(22):5243. https://doi.org/10.3390/molecules25225243. PMID: 33187049; PMCID: PMC7697716.
2. Nardarajah D. Hesperidin-A short review. Research J Pharm Tech. 2014; 7(1):78-80.
3. Hostetler GL, Ralston RA, Schwartz SJ. Flavones: Food sources, bioavailability, metabolism, and bioactivity. Adv Nutr. 2017; 8(3):423-35. https://doi.org/10.3945/an.116.012948. PMID: 28507008; PMCID: PMC5421117.
4. Liu W, Feng Y, Yu S, Fan Z, Li X, Li J, Yin H. The flavonoid biosynthesis network in plants. Int J Mol Sci. 2021; 22(23):12824. https://doi.org/10.3390/ijms222312824. PMID: 34884627; PMCID: PMC8657439.
5. Tapas A, Sakarkar D, Kakde R. The chemistry and biology of bioflavonoids. Research J Pharm Tech. 2008; 1(3):132-43.
6. Azuma K, Ippoushi K, Ito H, Higashio H, Terao J. Combination of lipids and emulsifiers enhances the absorption of orally administered quercetin in rats. J Agric Food Chem. 2002; 50(6):1706-12. https://doi.org/10.1021/jf0112421. PMID: 11879062.
7. Oliveira EJ, Watson DG, Grant MH. Metabolism of quercetin and kaempferol by rat hepatocytes and the identification of flavonoid glycosides in human plasma. Xenobiotica. 2002; 32(4):279-87. https://doi.org/10.1080/00498250110107886. PMID: 12028662.
8. Dajas F, Rivera-Megret F, Blasina F, Arredondo F, Abin-Carriquiry JA, Costa G, *et al.* Neuroprotection by flavonoids. Braz J Med Biol Res. 2003; 36(12):1613-20. https://doi.org/10.1590/s0100-879x2003001200002. PMID: 14666245.
9. Embi N, Rylatt DB, Cohen P. Glycogen synthase kinase-3 from rabbit skeletal muscle. Separation from cyclic-AMP-dependent protein kinase and phosphorylase kinase. Eur J Biochem. 1980; 107(2):519-27. https://doi.org/10.1111/j.1432-1033.1980.tb06059.x. PMID: 6249596.
10. Perez-Costas E, Gandy JC, Melendez-Ferro M, Roberts RC, Bijur GN. Light and electron microscopy study of glycogen synthase kinase-3beta in the mouse brain. PLoS One. 2010; 5(1):e8911. https://doi.org/10.1371/journal.pone.0008911. PMID: 20111716; PMCID: PMC2811740.
11. Woodgett JR. Molecular cloning and expression of glycogen synthase kinase-3/factor A. EMBO J. 1990; 9(8):2431-8. https://doi.org/10.1002/j.1460-2075.1990.tb07419.x. PMID: 2164470; PMCID: PMC552268.

12. Ferrer I, Barrachina M, Puig B. Glycogen synthase kinase-3 is associated with neuronal and glial hyperphosphorylated tau deposits in Alzheimer's disease, Pick's disease, progressive supranuclear palsy and corticobasal degeneration. Acta Neuropathol. 2002; 104(6):583-91. https://doi.org/10.1007/s00401-002-0587-8. PMID: 12410379.
13. Pandey GN, Dwivedi Y, Rizavi HS, Teppen T, Gaszner GL, Roberts RC, *et al*. GSK-3beta gene expression in human postmortem brain: regional distribution, effects of age and suicide. Neurochem Res. 2009; 34(2):274-85. https://doi.org/10.1007/s11064-008-9770-1. PMID: 18584322.
14. Darshit BS, Balaji B, Rani P, Ramanathan M. Identification and *in vitro* evaluation of new leads as selective and competitive glycogen synthase kinase-3β inhibitors through ligand and structure-based drug design. J Mol Graph Model. 2014; 53:31-47. https://doi.org/10.1016/j.jmgm.2014.06.013. PMID: 25064440.
15. Reddy R, Venkateswarulu TC, Babu JD, Devi SN. Homology modelling, simulation and docking studies of tau-protein kinase. Research J Pharm Tech. 2014; 7(3):376-88.
16. Busciglio J, Lorenzo A, Yeh J, Yankner BA. Beta-amyloid fibrils induce tau phosphorylation and loss of microtubule binding. Neuron. 1995; 14(4):879-88. https://doi.org/10.1016/0896-6273(95)90232-5. PMID: 7718249.
17. Takashima A, Noguchi K, Sato K, Hoshino T, Imahori K. Tau protein kinase I is essential for amyloid beta-protein-induced neurotoxicity. Proc Natl Acad Sci USA. 1993; 90(16):7789-93. https://doi.org/10.1073/pnas.90.16.7789. PMID: 8356085; PMCID: PMC47228.
18. Alvarez G, Muñoz-Montaño JR, Satrústegui J, Avila J, Bogónez E, Díaz-Nido J. Lithium protects cultured neurons against beta-amyloid-induced neurodegeneration. FEBS Lett. 1999; 453(3):260-4. https://doi.org/10.1016/s0014-5793(99)00685-7. PMID: 10405156.
19. Pietta PG. Flavonoids as antioxidants. J Nat Prod. 2000; 63(7):1035-42. https://doi.org/10.1021/np9904509. PMID: 10924197.
20. Alanbaki AA, AL-Mayali HM, AL-Mayali HK. Ameliorative effect of quercetin and hesperidin on antioxidant and histological changes in the testis of etoposide-induced adult male rats. Research J Pharm Tech. 2018; 11(2):564-74. https://doi.org/10.5958/0974-360X.2018.00105.1.
21. Al-Khayri JM, Sahana GR, Nagella P, Joseph BV, Alessa FM, Al-Mssallem MQ. Flavonoids as potential anti-inflammatory molecules: A review. Molecules. 2022; 27(9):2901. https://doi.org/10.3390/molecules27092901. PMID: 35566252; PMCID: PMC9100260.
22. Frandsen JR, Narayanasamy P. Neuroprotection through flavonoid: Enhancement of the glyoxalase pathway. Redox Biol. 2018; 14:465-73. https://doi.org/10.1016/j.redox.2017.10.015. PMID: 29080525; PMCID: PMC5680520.
23. Bhat R, Xue Y, Berg S, Hellberg S, Ormö M, Nilsson Y, *et al*. Structural insights and biological effects of glycogen synthase kinase 3-specific inhibitor AR-A014418. J Biol Chem. 2003; 278(46):45937-45. https://doi.org/10.1074/jbc.M306268200. PMID: 12928438.
24. Carter YM, Kunnimalaiyaan S, Chen H, Gamblin TC, Kunnimalaiyaan M. Specific glycogen synthase kinase-3 inhibition reduces neuroendocrine markers and suppresses neuroblastoma cell growth. Cancer Biol Ther. 2014; 15(5):510-5. https://doi.org/10.4161/cbt.28015. PMID: 24521712; PMCID: PMC4026073.
25. Schrödinger LLC. Schrödinger release 2021-1: protein preparation wizard. Epic Impact Prime. New York: Schrödinger LLC; 2021.
26. Halgren TA, Murphy RB, Friesner RA, Beard HS, Frye LL, Pollard WT, *et al*. Glide: a new approach for rapid, accurate docking and scoring. 2. Enrichment factors in database screening. J Med Chem. 2004; 47(7):1750-9. https://doi.org/10.1021/jm030644s. PMID: 15027866.
27. Reddy SCH, Reddy SKG, Mahto MK, Kunala P, Kanth CR. *In silico* design and discovery of some novel ache inhibitors for the treatment of Alzheimer's disorder. Research J Pharm and Tech. 2012; 5(3):424-7.
28. Malathi R, Dsouza V, Puja, Rithika R, Sneha P. Molecular docking of fisetin as a multi-target drug in the treatment of Alzheimer's disease. Res J Pharm Tech. 2023; 16(12):5813-7. https://doi.org/10.52711/0974-360X.2023.00941
29. Sawhney SK, Narayan C, Mishra A, Singh M, Kaur A. Molecular docking, ADME and toxicity study of Dibenzo-α-pyrone derivatives for GABA and NMDA receptors for their antiepileptic activity. Res J Pharm Tech. 2024; 17(1):340-6. https://doi.org/10.52711/0974-360X.2024.00053
30. Kesavan K, Jayanthi S. Structure-based virtual screening and molecular dynamics studies to identify novel APE1 inhibitor from seaweeds as an anti-glioma agent. Res J Pharm Tech. 2017; 10(8):2474-8. https://doi.org/10.5958/0974-360X.2017.00437.1
31. Mandel JL, Pearson ML. Insulin stimulates myogenesis in a rat myoblast line. Nature. 1974; 251(5476):618-20. https://doi.org/10.1038/251618a0. PMid:4421831
32. Nga NTH, Ngoc TTB, Trinh NTM, Thuoc TL, Thao DTP. Optimization and application of MTT assay in determining the density of suspension cells. Anal Biochem. 2020; 610:113937. https://doi.org/10.1016/j.ab.2020.113937. PMid:32896515
33. Bahuguna A, Khan I, Bajpai VK, Kang SC. MTT assay to evaluate the cytotoxic potential of a drug. Bangladesh J Pharmacol. 2017; 12:115-8. https://doi.org/10.3329/bjp.v12i2.30892
34. Radhakrishnan M, Ramesh S. *In vitro* glucose uptake activity of traditional polyherbal formulation in skeletal muscle Cells. Res J Pharm Tech. 2016; 9(5):506-8. https://doi.org/10.5958/0974-360X.2016.00094.9

35. Liu Y, Encinas M, Comella JX, Aldea M, Gallego C. Basic helix-loop-helix proteins bind to TrkB and p21(Cip1) promoters linking differentiation and cell cycle arrest in neuroblastoma cells. Mol Cell Biol. 2004; 24(7):2662-72. https://doi.org/10.1128/MCB.24.7.2662-2672.2004. PMid:15024057 PMCid: PMC371129
36. Cheung YT, Lau WK, Yu MS, Lai CS, Yeung SC, So KF, *et al*. Effects of all-trans-retinoic acid on human SH-SY5Y neuroblastoma as *in vitro* model in neurotoxicity research. Neurotoxicology. 2009; 30(1):127-35. https://doi.org/10.1016/j.neuro.2008.11.001. PMid:19056420
37. Strittmatter SM, Vartanian T, Fishman MC. GAP-43 is a plasticity protein in neuronal form and repair. J Neurobiol. 1992; 23(5):507-20. https://doi.org/10.1002/neu.480230506. PMid:1431834
38. Kim S, Ghil SH, Kim SS, Myeong HH, Lee YD, Suh-Kim H. Overexpression of neurogenin1 induces neurite outgrowth in F11 neuroblastoma cells. Exp Mol Med. 2002; 34(6):469-75. https://doi.org/10.1038/emm.2002.65 PMid:12526089
39. Constantinescu R, Constantinescu AT, Reichmann H, Janetzky B. Neuronal differentiation and long-term culture of the human neuroblastoma line SH-SY5Y. J Neural Transm Suppl. 2007; 72:17-28. https://doi.org/10.1007/978-3-211-73574-9_3 PMid:17982873
40. Agholme L, Lindström T, Kågedal K, Marcusson J, Hallbeck M. An *in vitro* model for neuroscience: differentiation of SH-SY5Y cells into cells with morphological and biochemical characteristics of mature neurons. J Alzheimers Dis. 2010; 20(4):1069-82. https://doi.org/10.3233/JAD-2010-091363. PMid:20413890
41. López-Carballo G, Moreno L, Masiá S, Pérez P, Barettino D. Activation of the phosphatidylinositol 3-kinase/Akt signaling pathway by retinoic acid is required for neural differentiation of SH-SY5Y human neuroblastoma cells. J Biol Chem. 2002; 277(28):25297-304. https://doi.org/10.1074/jbc.M201869200 PMid:12000752
42. Karthika S, Kannappan N, Suriyaprakash TNK. Effect of medicinal plants on amyloid β1-42 Intoxicated SH-SY5Y cell Lines - As neuroprotective evaluation. Res J Pharm Tech. 2020; 13(7):3351-5. https://doi.org/10.5958/0974-360X.2020.00595.8
43. Ranjithkumar R, Alhadidi Q, Shah ZA, Ramanathan M. Tribulusterine containing *Tribulus terrestris* extract exhibited neuroprotection through attenuating stress kinases mediated inflammatory mechanism: *In vitro* and *In vivo* studies. Neurochem Res. 2019; 44(5):1228-42. https://doi.org/10.1007/s11064-019-02768-7. PMid:30863969